

A Markov Decision Model for Adaptive Scheduling of Stored Scalable Videos

Chao Chen, *Student Member, IEEE*, Robert W. Heath Jr., *Fellow, IEEE*,
Alan C. Bovik, *Fellow, IEEE*, and Gustavo de Veciana, *Fellow, IEEE*

Abstract—We propose two scheduling algorithms that seek to optimize the quality of scalably coded videos that have been stored at a video server before transmission. The first scheduling algorithm is derived from a Markov decision process (MDP) formulation developed here. We model the dynamics of the channel as a Markov chain and reduce the problem of dynamic video scheduling to a tractable Markov decision problem over a finite-state space. Based on the MDP formulation, a near-optimal scheduling policy is computed that minimizes the mean square error. Using insights taken from the development of the optimal MDP-based scheduling policy, the second proposed scheduling algorithm is an online scheduling method that only requires easily measurable knowledge of the channel dynamics, and is thus viable in practice. Simulation results show that the performance of both scheduling algorithms is close to a performance upper bound also derived in this paper.

Index Terms—Scheduling algorithm, videos transport, wireless communication.

NOMENCLATURE

F^{intra}	Number of frames in an intraperiod.
F^{GOP}	Number of frames in a GOP.
L	Number of MGS layers.
z_t	The amount of received data for the frame played out at t .
ω_ℓ^k	The amount of data in the ℓ th layer of a type- k frame.
d_ℓ	The distortion when the ℓ th layer is correctly received.
$d^k(z_t)$	The rate-distortion model for type- k frames.
$\hat{d}^k(z_t)$	The concave envelopes of $d^k(z_t)$.
X_t	The transmission bit rate at t .
Y_t	The packet error rate at t .
R_t	The channel throughput at t .
r^{avg}	The average channel throughput.
C_t	The channel state at t .
V_t	The buffer state at t .
S_t	The system state at t .

Manuscript received September 10, 2012; revised December 24, 2012; accepted February 05, 2013. Date of publication March 27, 2013; date of current version May 31, 2013. This work was supported in part by Intel Inc. and Cisco Corporation under the VAWN program. This paper was recommended by Associate Editor E. Steinbach.

The authors are with the Department of Electrical and Computer Engineering, The University of Texas at Austin, Austin, TX 78712-0240 USA (e-mail: chao.chen@utexas.edu; rheath@ece.utexas.edu; bovik@ece.utexas.edu; gustavo@ece.utexas.edu).

Color versions of one or more of the figures in this paper are available online at <http://ieeexplore.ieee.org>.

Digital Object Identifier 10.1109/TCSVT.2013.2254896

I. INTRODUCTION

THE VARIATION of wireless channel capacity and tight delay constraints make the delivery of video difficult. Although adaptive transmission strategies, such as adaptive video data scheduling, can be employed, deriving the optimal adaptive transmission policy is difficult because the transmission strategies taken at different time are coupled with each other via receiver buffer state. Furthermore, due to the nature of predictive video coding algorithms, a video frame can be decoded only when its predictors have been received. Hence, the prediction structure of the video codec enforces a partial order on the transmissions of the video packets, which limits the flexibility of adaptive video transmission.

Scalable video coding (SVC) is one approach to enable flexible video transmission over channels with varying throughput [1], [2]. An SVC video encoder produces a layered video stream that contains a base layer and several enhancement layers. If the throughput is low, the transmitter can choose to transmit the base layer only, which provides a moderate, but acceptable, degree of visual quality at the receiver. If the channel conditions improve, the transmitter can transmit one, or more, enhancement layers to further improve the visual quality. Conceptually, SVC provides a means to adapt the data rate for wireless video transmission. The wireless transmitter can adapt the data rate by selectively scheduling video data associated with various layers for transmission rather than transcoding the video sequence into a different rate.

Designing scalable video scheduling algorithms for wireless channels is a complex task. The scheduling policy depends not only on the channel conditions, but also on the receiver buffer state. For example, if the receiver has successfully buffered base layer data over many frames, the scheduler could choose to transmit some enhancement layer data to improve the video quality even if the throughput is low. At any time, the scheduling decision will determine the receiver buffer state which, in turn, affects the future scheduling decisions. Therefore, adaptive video data scheduling is a sequential decision problem. The most natural way to address such problems is to model the dynamics of the channel as a finite-state Markov chain (FSMC) and to employ a Markov decision process (MDP)-based formulation to study scheduling methods. For stored video transmission, however, directly determining an optimal scheduling policy using an MDP formulation is not possible, because the system state space is infinitely large (Section III-A). Moreover, in a practical wireless network, a

model for the dynamics of the channel states is not typically available, which limits the applicability of this approach.

A. Contributions

The objective of this paper is to leverage the MDP framework to develop practical scheduling algorithms and optimize the receiver video quality for stored scalable video transmission over wireless channels. First, we propose a tractable MDP formulation based on a reasonable approximation of the state space. Near-optimal scheduling policies can be derived from this MDP formulation. Second, we propose a scheduling algorithm that substantially simplifies the MDP-based scheduling policy as it requires only limited information regarding the channel state dynamics. Third, we prove an upper bound on the achievable video quality of all possible scheduling algorithms. Finally, we provide simulation results that show, under different channel conditions, the performance of the proposed scheduling algorithms is indeed very close to the upper bound.

Our contributions are summarized in the following.

- 1) *An MDP formulation is proposed to facilitate the design of adaptive scheduling policies for stored video transmission.* In this paper, we focus on stored video transport, where video sequences have been encoded and stored on a video server before transmission. This is quite different from real-time video transmission where video frames are generated in real time. The video scheduler can select any data from the video sequence and send the data to the receiver buffer. Thus, the number of possible receiver buffer states can be effectively regarded as infinite. Because the performance of the scheduling policy depends on the receiver buffer state, the policy needs to be optimized over an infinitely large state space and the scheduling problem is intractable. In this paper, by applying reasonable restrictions on the set of scheduling policies considered in our MDP formulation, we prove that optimizing the transmission policy is equivalent to solving a semi-Markov decision problem on a finite-state set (Section III). Based on this result, near-optimal scheduling policies can be derived using the proposed MDP formulation.
- 2) *A near-optimal and online scheduling algorithm is proposed.* In most cases, models for channel dynamics are not available. By simplifying the channel model and the scheduling decision of the MDP formulation, we devise an online scheduling algorithm which, unlike the MDP-based policy, only requires limited measurable knowledge of the channel dynamics. Simulation results show that the proposed online algorithm performs nearly as well as the MDP-based scheduling policy.
- 3) *Performance optimality is justified.* To assess the performance of the proposed scheduling algorithms, an upper bound on the achievable video quality for adaptive scheduling is proved. Simulation results show that both the MDP-based scheduling policy and the proposed online scheduling policy perform close to the upper bound.

B. Related Work

Adaptive video data scheduling is an important topic of research [3]–[12]. In [3], adaptive video transmission over a packet erasure channel was studied by modeling the buffer state as a controlled Markov chain. In [4], an average-rate-constrained MDP formulation was proposed to optimize the quality of error-concealed videos at the receiver. For time-varying wireless channels, the amount of data that can be scheduled during a time slot is limited by the channel capacity at the slot. Only considering the constraint of the average transmission rate is insufficient. In [5], an MDP-based scheduling algorithm was proposed for video transmission over packet loss networks. This paper was further extended for wireless video streaming in [6], where the wireless channel was modeled as a binary symmetric channel. This channel model can only be justified for fast-fading channels, where the coherence time is much less than the delay constraint. In that case, interleaving can be applied without violating the delay constraint, and the channel will appear as an i.i.d. channel. For slow-fading channels, such as those considered here, the bit error rate cannot be modeled as a constant. In [7], adaptive scheduling of scalable videos was studied using an MDP model. The reward of each frame slot was defined as a utility function of the buffer state and the transmission rate. A foresighted scheduling policy was derived to maximize the long-term reward over all frame slots. Comparing with a scheduling method that myopically maximizes the reward of each individual frame slot, the proposed scheduling algorithm improved the video quality significantly. In [8]–[11], reinforcement learning frameworks were proposed for wireless video transmission. Their proposed algorithms were based on MDP using a discounted-reward maximization formulation. The transmitter learns the characteristics of the channel and the video sequence during the transmission process. The scheduling policy is updated according to the learned characteristics. In our previous work [12], an infinite-horizon average-reward maximization MDP formulation was proposed. The channel characteristics, unlike in this paper, were assumed to be known.

The most closely related prior work is [6]–[11], which focus on scalable video transmission over wireless channels. Our paper contrasts with these as follows.

- 1) *An infinite-state space problem for stored video streaming:* For real-time video transmission, the number of video frames that are ready for transmission is finite because later frames have not yet been generated at the video source. Therefore, the scheduler only needs to select data from a finite set of frames [6]–[10]. In this paper, we focus on stored video streaming, where all the video frames have been encoded before transmission. In this case, the scheduler is allowed to select data from any video frame and the number of possible receiver buffer states is therefore infinitely large. In this paper, we construct a finite-state MDP model and show that the optimal policy derived from this MDP model is also optimal for the original infinite-state problem.
- 2) *Channel model:* We focus on slow-fading wireless channels experienced by pedestrian users. In the channel

model of [6], the bit error probability of the channel was assumed constant. This assumption can only be justified for fast-fading channels, where the channel coherence time is much less than the delay constraint in video applications. In that case, interleaving can be applied without violating the delay constraint, and the channel will appear to have i.i.d. bit errors. For slow-fading channels, where the coherence time is much longer, it is impossible to apply interleaving over many coherence periods due to the delay constraint. In this case, i.i.d. models are no longer suitable because they do not capture information regarding channel variations. In contrast, the algorithm proposed in this paper explicitly considers channel state variation in scheduling.

- 3) *Optimization objective*: Most of the existing MDP-based scheduling algorithms are based on a *utility* function as the optimization objective [7]–[10]. The utility function is usually written as a weighted sum of the transmission bit rate and the amount of buffered data. The weights assigned to each component of the summation, to some extent, reflect their importance, but are heuristically chosen. The resulting utility function cannot accurately indicate the quality of played out frames. Here, instead of optimizing a utility function, we directly optimize the quality of the video frame played out in each frame slot.
- 4) *Nonavailability of channel state dynamics*: In a practical wireless video transmission application, models for the dynamics of the channel state are typically unavailable. To address this problem, a reinforcement learning algorithm can be employed to learn a good policy from making wrong scheduling actions [8]–[10]. Video quality, however, will be degraded during the learning period, which can be as long as tens of seconds. We propose an adaptive alternative to such reinforcement learning methods that only uses the channel coherence time and current channel throughput which are easy to measure in practice. The performance of the proposed algorithm is very close to a derived performance upper bound.

C. Organization of This Paper

This paper is organized as follows. The system model is introduced in Section II. The assumptions we make about the video codec and the rate-distortion model are described in Section II. In Section III, the MDP formulation and the performance upper bound are proposed. A near-optimal online scheduling algorithm is introduced and validated by simulations in Section IV. Section V concludes the paper.

II. SYSTEM MODEL

In this section, we describe the wireless video system to be considered. Then, we present our video codec configuration and introduce the rate-distortion model.

We briefly introduce some notation used in the paper. \mathbf{A} and \mathbf{a} are examples of a matrix and a vector, respectively. \mathcal{A} is a set. $|\mathcal{A}|$ is the cardinality of set \mathcal{A} . $\lceil \cdot \rceil$ is the ceiling function. $\mathbb{P}(\cdot)$ is the probability measure and $\mathbb{E}[\cdot]$ is

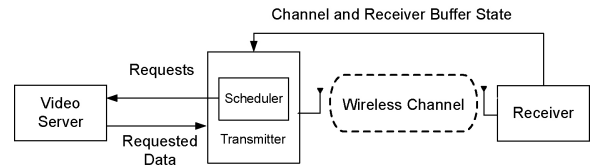


Fig. 1. Dynamic scheduling system for wireless video transmission.

the expectation. $\mathbb{N} = \{0, 1, 2, \dots\}$ is the set of nonnegative integers. Other frequently used notations are summarized in the Nomenclature.

A. System Overview

We consider a time-slotted system that transmits scalable videos over a slow-fading wireless channel. The video sequence is encoded with a quality-scalable video encoder and is stored in a video server. The video server transmits video data to a mobile user via a wireless transmitter. The duration of each frame ΔT is called a frame slot. In each frame slot, the server sends some video data upon request of a scheduler at the wireless transmitter. This data are packetized at the wireless transmitter for physical layer transmission. The channel and receiver buffer state is sent to the scheduler via a feedback channel with negligible delay. The scheduler operates according to a policy that maps the channel and receiver buffer state to the scheduling action (Fig. 1).

In wireless communication systems such as 3GPP, using the technique of limited feedback, channel state information measured at the receiver can be fed back to the transmitter via a control channel [13]–[15]. The delay of the feedback channel is typically much smaller than a frame slot. For example, the feedback delay in 3GPP is 6 ms [15], which is much shorter than the 33 ms frame slot of 30 frames/s videos. Similarly, the video packets received in each slot can also be acknowledged via a control channel with negligible delay. Therefore, similar to most of existing MDP formulations such as [7]–[10], we assume the feedback is instantaneous. For the case where feedback delay is longer than a frame slot [16].

We assume that the link between the video server and the wireless transmitter is not the bottleneck for transmission to the mobile. Thus, from the perspective of the wireless transmitter, the whole video sequence is available for transmission. We also assume that the physical layer channel state information is available at the transmitter and that the modulation and coding scheme is determined by a given physical layer link-adaptation policy.

B. Video Codec Configuration

We assume that the video sequence is encoded by an H.264/SVC video encoder. The video frames are uniformly partitioned into intraperiods. Every intraperiod has F^{intra} frames and is further partitioned uniformly into group of pictures (GOPs). Each GOP has F^{GOP} frames. They are encoded using the “Hierarchical B” prediction structure [1], in which video frames are hierarchically organized into T temporal layers as shown in Fig. 2. The last frame in each GOP is called a *key picture*. These key pictures form the 0th

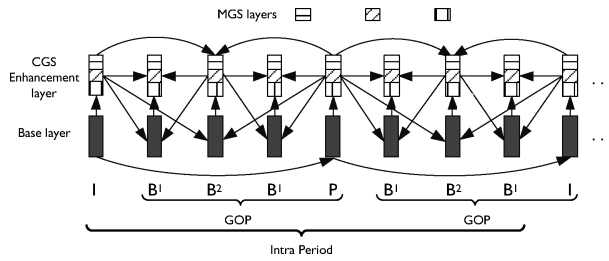


Fig. 2. Encoder prediction structure considered in this paper. The prediction order is indicated by arrows. The length of intraperiod is $F^{\text{intra}} = 8$ and the GOP length is $F^{\text{GOP}} = 4$. The CGS enhancement layer is partitioned into three MGS layers.

temporal layer. There are two types of key pictures: I frames and P frames. The first picture in an intraperiod is called an I frame, which is encoded without referring other frames. The other key pictures are P frames. Each P frame is encoded using a preceding key pictures as reference. All the frames in higher temporal layers are B frames. A B frame in the τ th temporal layer is encoded using the preceding frame and the succeeding frame in the lower temporal layers as reference. In the following, we call a frame in the τ th temporal layer a B^τ frame, where $\tau \geq 1$ (Fig. 2).

Every frame is encoded into a base layer and a coarse grain scalability (CGS) layer. The base layer of an I frame is encoded independently. The base layer of a P frame is predictively encoded using the base layer of the preceding key picture. The CGS layer of all key pictures is predictively encoded using their respective base layers. For a B frame, its base layer is encoded using the CGS layers of its reference frames. Its CGS layer is encoded using both its base layer and the CGS layers of its reference frames (see Fig. 2).

The CGS layer of each frame is further partitioned into L MGS layers. Each MGS layer contains a portion of the CGS layer data. Thus, the more MGS layers are received, the higher decoding quality can be achieved. In the following, we call the base layer and the MGS layers *quality layers*. We focus on adaptive scheduling of the quality layers in a video stream. The temporal scalability is not exploited.

In this paper, we only consider one CGS enhancement layer. In H.264/SVC, multiple CGS layer is supported and each CGS layer can be partitioned into several MGS layers. The switch between CGS layers, however, is only possible at instantaneous decoder refresh (IDR) frames, which are separated from each other by several intraperiods. Therefore, CGS cannot support frame-by-frame rate adaptation. Since the coherence time of wireless channels is much shorter than a intraperiod, flexible rate adaptation can only be achieved by MGS, which allows us to vary the number of quality layer for each frame. Here, we consider frame-by-frame adaptive scheduling of the MGS layers within a single CGS enhancement layer. For the video streams that contain multiple CGS enhancement layers, our scheduling algorithm can be applied to conduct adaptation in one of the CGS enhancement layers while treating all lower layers as the base layer. In the following, we call the MGS layers *enhancement layers*.

Each frame has a playout deadline at the receiver. In the following, frames whose deadlines have expired are called

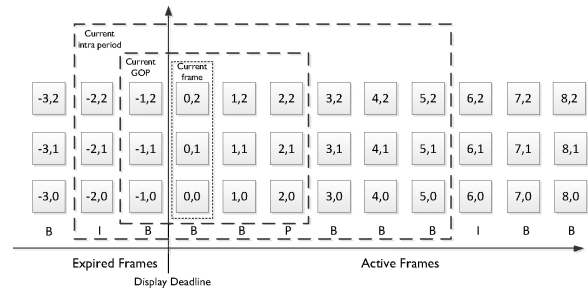


Fig. 3. Indices of data units when three quality layers are considered. At the beginning of each time slot, the frame with index $f = 0$ is played out. All the data units in the figure shift left.

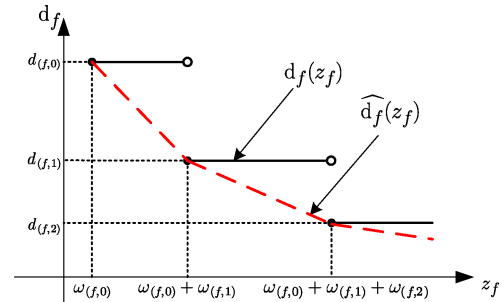


Fig. 4. Rate-distortion function $d_f(z_f)$ for the f th frame. The rate-distortion function $d_f(z_f)$ is piecewise constant and right-continuous (solid). Its convex envelope $\hat{d}_f(z_f)$ is also shown (dashed).

expired frames; otherwise, they are said to be active frames. The first active frame is called the “current frame.” The GOP that contains the current frame is called the “current GOP.” The intraperiod that contains the current frame is called the “current intraperiod” (see Fig. 3). The frames in the current GOP are decoded together when the first frame of the GOP is displayed. At any point in time, frames are indexed relative to the current frame as shown in Fig. 3. Each data unit is also tagged with a layer index ℓ . The index for base layer is $\ell = 0$ and the enhancement layers are index from 1 to L . The video data in the ℓ th layer of the f th frame are called the (f, ℓ) th video data unit.

C. Rate-Distortion Model

Let z_f be the amount of received data for the f th frame. The rate-distortion function $d_f(z_f)$ captures the quality of the frame when it is decoded, given all its predictors have been received. Let $\omega_{(f,\ell)}$ be the amount of data in the (f, ℓ) th data unit and $d_{(f,\ell)}$ be the distortion measured in mean square error (MSE) if the 0th \sim ℓ th layers have been correctly received. As shown in Fig. 4, since a data unit can be decoded only when all its associated data has been received, $d_f(z_f)$ is a piecewise constant and right-continuous function with jumps at $z_f = \sum_{\ell=0}^m \omega_{(f,\ell)}$, $m = 0, 1, \dots, L$. Thus, $d_{(f,\ell)}$ and $\omega_{(f,\ell)}$ characterize $d_f(z_f)$.

In a real video sequence, for a given layer ℓ , the rate-distortion characteristics $\omega_{(f,\ell)}$ and $d_{(f,\ell)}$ vary across frames. Let $\mathcal{K} = \{I, P, B^1, \dots, B^T\}$ be the set of frame types. We model $\omega_{(f,\ell)}$ of type k frames as i.i.d. realizations of a random variable Ω_ℓ^k , where $k \in \mathcal{K}$. Then, we use $\omega_\ell^k = \mathbb{E}[\Omega_\ell^k]$ as an

estimate of $\omega_{(f,\ell)}$. Similarly, for a given layer ℓ , we model $d_{(f,\ell)}$ as i.i.d. realizations of a random variable D_ℓ . We use $d_\ell = \mathbb{E}[D_\ell]$ as an approximation of $d_{(f,\ell)}$. Here, we choose not to distinguish the frame types when modeling $d_{(f,\ell)}$. In a typical H.264/SVC video stream, the quantization parameters (QPs) of the encoder are usually configured to minimize visually annoying quality fluctuations across different types of frames. Hence, for simplicity, we use a single random variable D_ℓ to model $d_{(f,\ell)}$ for all types of frames.

Our rate-quality models $d^k(z_f)$ for type- k frames are constructed as piecewise constant functions with jumps at $z_f = \sum_{\ell=0}^m \omega_\ell^k$, $m = 0, 1, \dots, L$. For stored video transmission, which is the focus of this paper, since the transmitted video has already been encoded, the size of each data unit is thus available. The parameters $\{\omega_\ell^k, k \in \mathcal{K}\}$ can thus be estimated by averaging across frames. If the distortion characteristic $d_{(f,\ell)}$ is calculated when the video is encoded, the parameter d_ℓ can also be estimated by averaging $d_{(f,\ell)}$ across frames. If $d_{(f,\ell)}$ is not available, d_ℓ needs to be estimated online. For example, the quality of frames that have been decoded at the receiver can be fed back to the transmitter for estimation.

D. Streaming Setup

We focus on scheduling for a slow-fading channel. By slow fading, we mean that the coherence time of the channel is less than the duration of an intraperiod and larger than a frame slot. Assuming the mobile users are moving in a 1.5 m/s walking speed and the carrier frequency is 2 GHz, the Doppler spread is about 10 Hz. The coherence time is about 100 ms. A typical intraperiod duration is about 1 s and a frame slot is about 30 ms. Hence, for pedestrian video users, wireless channels are slow fading.

As the channel state is stable during each frame slot, the scheduling decision is made on a frame-by-frame basis. At the beginning of each frame slot, a frame is played out, and video data units are scheduled for transmission. The scheduling action is defined as a set of ordered video data units

$$\mathcal{U} = \{(f_1, \ell_1), (f_2, \ell_2), \dots, (f_{|\mathcal{U}|}, \ell_{|\mathcal{U}|})\}. \quad (1)$$

When scheduling action \mathcal{U} is taken, the associated data units are transmitted sequentially. Each scheduled data unit is packetized into physical layer packets and each packet is repeatedly transmitted, i.e., if packet error occurs, until acknowledged.

In this paper, we consider data unit level scheduling. If a packet-level rate-quality model such as [10] is available, our MDP formulation can also be used to optimize the packet-level scheduling policy.

III. MDP-BASED MODEL

In this section, we propose an MDP-based model to determine the near-optimal scheduling policy. To that end, we describe the scheduler's state space and the policies to be considered. We then show how to reduce the scheduling problem to a finite-state Markov decision problem using reasonable approximations. With the MDP-based model, the optimal scheduling policy is computed offline via value iteration. The computed policy can then be used for online

adaptive scheduling. To validate the optimality of the MDP-based scheduling policies, we develop a performance upper bound at the end of this section.

A. Scheduling Policy and State Space

Considering all possible scheduling actions makes defining the scheduling policy and representing the buffer state unmanageably complex. On one hand, to capture the buffer state, the frame index and the layer index of each received data unit need to be recorded. If we assume an infinite playback buffer, the number of received data units is not bounded. So we cannot represent all possible buffer states using a finite-dimensional space. On the other hand, not all possible scheduling policies need to be considered. For example, a quality layer of a frame should not be transmitted before the lower quality layers of the frame because an SVC decoder cannot decode a quality layer without the lower layers [1]. Thus, we need only consider those scheduling strategies that are not dominated and have potential to achieve good performance.

Specifically, we consider scheduling policies under the following assumptions.

Assumption 1: The scheduler always schedules the base layer data unit of a frame for transmission after the base layer data unit(s) of the reference frame(s). The scheduler always schedules the enhancement layer data unit of a frame for transmission after the data units of the lower layers.

Assumption 2: The scheduler always schedules enough amount of data such that the transmitter is kept transmitting during the whole slot.

Assumption 3: We define three sets of data units: \mathcal{W}^{pre} , \mathcal{W} , and $\mathcal{W}^{\text{post}}$. When the current frame is a B frame, the set \mathcal{W}^{pre} contains the data units with frame index $f \in [f^{\text{key}}, -1]$, where f^{key} is the frame index of the last expired key picture [see Fig. 5(a)]. When the current frame is a key picture, we define $\mathcal{W}^{\text{pre}} = \emptyset$. Note that \mathcal{W}^{pre} contains all the expired data units that are used to predict the frames in the current GOP. The set \mathcal{W} contains the data units in all quality layers of the first W frames, where W is larger than F^{GOP} . The set $\mathcal{W}^{\text{post}}$ contains the remaining active data units. We assume the scheduler first sends the data units in \mathcal{W} . Then, if all the data in \mathcal{W} and the predictors in \mathcal{W}^{pre} have been received, the policy greedily schedules all $1 + L$ quality layers of the frames in $\mathcal{W}^{\text{post}}$, i.e., starts transmitting the next frame in $\mathcal{W}^{\text{post}}$ only when all the layers of the preceding frame have been received [see Fig. 5(b)].

Assumption 4: In each slot, the scheduler only schedules data for the frames that have not been decoded. Assumption 1 ensures that the transmission order is compatible with the prediction order given in Section II-B. Assumption 2 ensures that the transmitter will not be idle during a slot and the capacity of the channel is fully exploited. Assumption 3 stems from the fact that, when many frames are buffered at the receiver, the scheduler can transmit more enhancement layers because there is sufficient time before the frames are played out. In other words, if all quality layers of W frames have been received, there is no need to worry about the channel capacity variation in the future. As will be discussed in Section III-C, this assumption helps to simplify the policy optimization

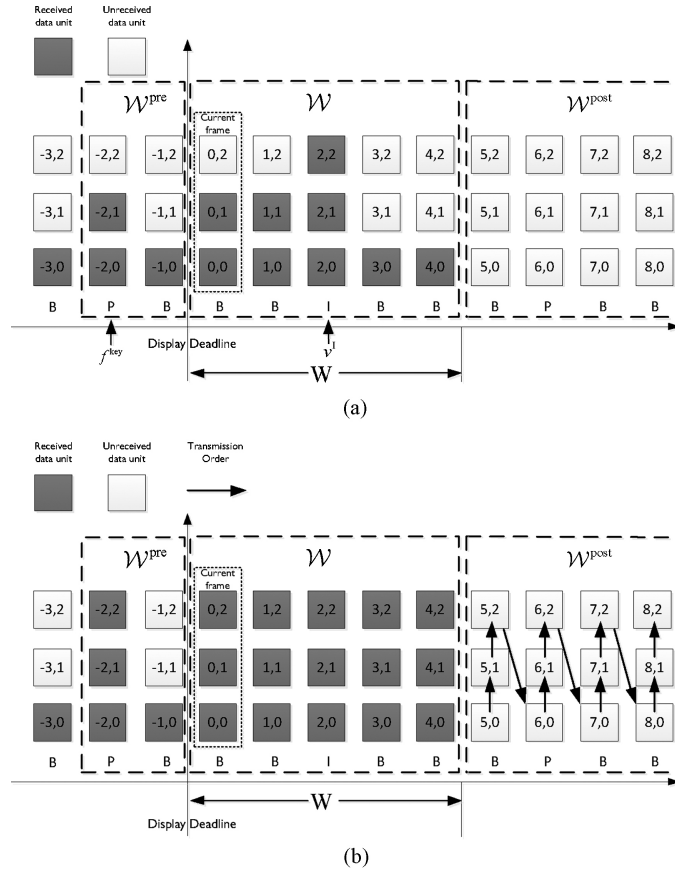


Fig. 5. (a) Receiver buffer state when $F^{\text{intra}} = 8$, $F^{\text{GOP}} = 4$, $L = 2$, and $W = 5$. $v^I = 2$, $\mathbf{v}^{\text{pre}} = (2, 1)$, $\mathbf{v}^{\text{W}} = (2, 2, 3, 1, 1)$, $\mathbf{v}^{\text{post}} = (0, 0, 0)$. Note that because some data units in \mathcal{W} have not been received, the data units in $\mathcal{W}^{\text{post}}$ are not sent. (b) Transmission order when the data in \mathcal{W} and the associated predictors in \mathcal{W}^{pre} have been received.

problem. It should be noted that policies under Assumption 3 are different from the sliding window policies defined in [5]. Indeed, our scheduling policy allows the transmitter to transmit data units outside the window. Assumption 4 ensures that the transmitter does not waste resources on the frames that have been decoded.

Remark 1: The window size W provides a tradeoff between complexity and optimality. The larger the window, the less constrained the control policy but the higher complexity.¹ We note that although the frames in the current GOP are played out sequentially, they are decoded together. According to Assumption 4, if $W \geq F^{\text{GOP}}$, the frames in \mathcal{W} have all been decoded and the scheduler cannot schedule any data from \mathcal{W} . Therefore, we set $W \geq F^{\text{GOP}}$.

We define the overall buffer state space \mathcal{V} via four sets \mathcal{V}^I , \mathcal{V}^{pre} , \mathcal{V}^{W} , and $\mathcal{V}^{\text{post}}$, where $\mathcal{V} = \mathcal{V}^I \times \mathcal{V}^{\text{pre}} \times \mathcal{V}^{\text{W}} \times \mathcal{V}^{\text{post}}$. The set \mathcal{V}^I records the types and playout deadlines of the frames in the buffer. The sets \mathcal{V}^{pre} , \mathcal{V}^{W} , and $\mathcal{V}^{\text{post}}$ describe the states of the frames in \mathcal{W}^{pre} , \mathcal{W} , and $\mathcal{W}^{\text{post}}$, respectively.

\mathcal{V}^I : We define v^I as the frame index of the active I frame with the earliest playout deadline. Since the prediction structure is assumed to be the same for all intraperiods, v^I determines the types and playout deadlines of all the frames in the receiver buffer.

\mathcal{V}^{pre} : If the current frame is a B frame, the state space \mathcal{V}^{pre} is defined as a vector $\mathbf{v}^{\text{pre}} = (b_{f^{\text{key}}}^{\text{pre}}, \dots, b_{-1}^{\text{pre}})$, where b_f^{pre} is the number of the received quality layers in the f th frame and f^{key} is the frame index of the last expired key picture. If the current frame is a key picture, $\mathcal{V}^{\text{pre}} = \emptyset$ and we define $\mathbf{v}^{\text{pre}} = -1$.

\mathcal{V}^{W} : Similar to \mathcal{V}^{pre} , we define the buffer state space for \mathcal{W} as a vector $\mathbf{v}^{\text{W}} = (b_0^{\text{W}}, \dots, b_{W-1}^{\text{W}})$, where b_f^{W} is the number of the received quality layers in the f th frame.

$\mathcal{V}^{\text{post}}$: The set $\mathcal{W}^{\text{post}}$ contains infinite number of frames. Therefore, recording the number of data units received for each frame is impossible. We note that, when Assumption 3 is enforced, the number of data units received in $\mathcal{W}^{\text{post}}$ must be nonincreasing in the frame index. Hence, we only need to record the total number of received data units for each layer. We define the buffer state space of $\mathcal{W}^{\text{post}}$ as a $1+L$ -dimensional vector $\mathbf{v}^{\text{post}} = (b_0^{\text{post}}, b_1^{\text{post}}, \dots, b_L^{\text{post}})$, where b_ℓ^{post} is the number of the received data units in the ℓ th layer of $\mathcal{W}^{\text{post}}$. Because the receiver buffer size is assumed to be large, i.e., essentially infinite, b_ℓ^{post} is unbounded. Thus, $\mathcal{V}^{\text{post}} = \mathbb{N}^{1+L}$, where $\mathbb{N} = \{0, 1, \dots, \infty\}$.

With the aforementioned definition, buffer state $\mathbf{v} = (v^I, \mathbf{v}^{\text{pre}}, \mathbf{v}^{\text{W}}, \mathbf{v}^{\text{post}})$ contains all the information that is relevant to the quality of frames in the receiver buffer.

¹In our simulations, we find that setting $W = 9$ is sufficient.

In [17] and [18], it is shown that a first-order FSMC can be used to describe the first-order channel state transition probabilities for Rayleigh fading channels. First-order FSMC models have also been validated in [19] and [20] by wireless channel measurements in urban areas. In our MDP-based model, we employ a first-order FSMC to describe the dynamics of the channel state.

We denote by x the transmission rate of the transmitter, i.e., the number of bits transmitted in a time slot ΔT . We denote by y the packet error rate of the channel. We define the channel state as $\mathbf{c} = (x, y)$. The channel state space is $\mathcal{C} = \{\mathbf{c}^1, \dots, \mathbf{c}^{|\mathcal{C}|}\}$, where $\mathbf{c}^i = (x^i, y^i)$ is the i th channel state. The state transition matrix \mathbf{P}^c is a $|\mathcal{C}| \times |\mathcal{C}|$ matrix with entry $\mathbf{P}_{i,j}^c = \mathbb{P}(\mathbf{c}^j | \mathbf{c}^i)$ being the transition probability from state \mathbf{c}^i to \mathbf{c}^j .

The system state space \mathcal{S} is defined as the product of the buffer state space \mathcal{V} and the channel state space \mathcal{C} . For each state $\mathbf{s} \in \mathcal{S}$, we define a feasible control set \mathcal{U}_s that contains all the scheduling actions [see (1)] complying with all the three assumptions. The state \mathbf{s} contains all the information about the receiver buffer and the channel. The transmitter must decide which action in \mathcal{U}_s to take in order to minimize the distortion. We define the scheduling policy $\mu(\cdot)$ as the mapping from the system state \mathbf{s} to an action in \mathcal{U}_s . Under given scheduling policy μ , the system state transit as a controlled Markov chain. The state transition probability $\mathbb{P}_\mu(\cdot | \cdot)$ is determined by the scheduling policy μ (see Appendix A for detail). In the following sections, we show how to optimize the scheduling policy $\mu(\cdot)$.

B. Optimization Objective

Since the channel condition is modeled as a random process, we denote by $(C_t, V_t, S_t)_{t \in \mathbb{N}}$ the random processes modeling channel, buffer, and system state, respectively. Accordingly, we denote $S = \lim_{t \rightarrow +\infty} S_t$. We define a function $d(\mathbf{s})$ of state \mathbf{s} as the estimated distortion of the frame that is played out at state \mathbf{s} .² Our aim is to find an optimal policy $\mu^*(\cdot)$ that minimizes the expectation of distortion, i.e.,

$$J_\mu = \mathbb{E}_\mu [d(S)] \quad (2)$$

where $\mathbb{E}_\mu[\cdot]$ is the expectation over the stationary distribution of the controlled Markov chain under policy μ .

We now introduce the definition of $d(\mathbf{s})$. If the displayed frame is a key picture (I frame or P frame), we estimate its distortion using the rate-distortion model in Section II-C as

$$d(\mathbf{s}) = \begin{cases} d^I(z(\mathbf{s})) & : \text{ for I frames} \\ d^P(z(\mathbf{s})) & : \text{ for P frames} \end{cases} \quad (3)$$

where $z(\mathbf{s})$ denotes the amount of received data for the displayed frame at state \mathbf{s} . If the displayed frame is a B frame, which is encoded using all the $1 + L$ layers of its reference frames as predictor, the distortion cannot be directly estimated using the rate-distortion model in Section II-C because the loss in the enhancement layers of its reference frames causes encoder–decoder predictor mismatch, which is also known as drift in SVC [1]. We employ the model proposed in [21] to take

²Since in each slot, a frame is played out before the scheduling actions are taken. Therefore, $d(\mathbf{s})$ is not a function of the actions taken at the state \mathbf{s} .

into account the distortion due to drift. Let $\{\widehat{v}_i^{\text{ref}}, i \in 1, 2\}$ denote the predictor for the B frame at the encoder, i.e., the pixel value of the i th reference frame with all the $1 + L$ layers. Let $\{\widetilde{v}_i^{\text{ref}}, i \in 1, 2\}$ be the predictor for the B frame at the decoder, i.e., the pixel value of the i th reference frame with all the received quality layers. The drift of the reference frame is thus $\epsilon_i^{\text{dft}} = \widetilde{v}_i^{\text{ref}} - v_i^{\text{ref}}$. In [21], it is shown that the MSE of a type- B^r frame can be estimated as

$$\widetilde{d}(\mathbf{s}) = d^{B^r}(z(\mathbf{s})) + \frac{1}{4} \mathbb{E}[(\epsilon_1^{\text{dft}})^2] + \frac{1}{4} \mathbb{E}[(\epsilon_2^{\text{dft}})^2] + \frac{1}{2} \mathbb{E}[\epsilon_1^{\text{dft}} \epsilon_2^{\text{dft}}] \quad (4)$$

where $d^{B^r}(z(\mathbf{s}))$ is the rate-distortion function defined in Section II-C and the other terms on the right-hand side are the distortions due to drift. Since $\mathbb{E}[(\epsilon_1^{\text{dft}} - \epsilon_2^{\text{dft}})^2] = \mathbb{E}[(\epsilon_1^{\text{dft}})^2] + \mathbb{E}[(\epsilon_2^{\text{dft}})^2] - 2\mathbb{E}[\epsilon_1^{\text{dft}} \epsilon_2^{\text{dft}}] \geq 0$, we have $\mathbb{E}[\epsilon_1^{\text{dft}} \epsilon_2^{\text{dft}}] \leq \frac{1}{2} \mathbb{E}[(\epsilon_1^{\text{dft}})^2] + \frac{1}{2} \mathbb{E}[(\epsilon_2^{\text{dft}})^2]$. Thus, $\widetilde{d}(\mathbf{s})$ is upper bounded by $d^{B^r}(z(\mathbf{s})) + \frac{1}{2} \mathbb{E}[(\epsilon_1^{\text{dft}})^2] + \frac{1}{2} \mathbb{E}[(\epsilon_2^{\text{dft}})^2]$. We use this upper bound as a proxy of the B frame's distortion in our MDP model. The function $d(\mathbf{s})$ is defined as

$$d(\mathbf{s}) = d^{B^r}(z(\mathbf{s})) + \frac{1}{2} \mathbb{E}[(\epsilon_1^{\text{dft}})^2] + \frac{1}{2} \mathbb{E}[(\epsilon_2^{\text{dft}})^2]. \quad (5)$$

The term $\mathbb{E}[(\epsilon_i^{\text{dft}})^2]$ is the estimate from the distortion of the reference frame as follows. Let v_i^{ref} be the original pixel value of the reference frame before encoding. The decoding error of the reference frame is thus $\epsilon_i^{\text{ref}} = v_i^{\text{ref}} - \widehat{v}_i^{\text{ref}} = (v_i^{\text{ref}} - \widehat{v}_i^{\text{ref}}) + (\widehat{v}_i^{\text{ref}} - v_i^{\text{ref}})$, where $\widehat{v}_i^{\text{ref}} - v_i^{\text{ref}} = \epsilon_i^{\text{dft}}$ is the distortion due to drift and $v_i^{\text{ref}} - \widehat{v}_i^{\text{ref}}$ is the distortion due to encoding. Assuming $\widehat{v}_i^{\text{ref}} - v_i^{\text{ref}}$ and $v_i^{\text{ref}} - \widehat{v}_i^{\text{ref}}$ are uncorrelated,³ we have $\mathbb{E}[(\epsilon_i^{\text{ref}})^2] = \mathbb{E}[(\epsilon_i^{\text{dft}})^2] + \mathbb{E}[(v_i^{\text{ref}} - \widehat{v}_i^{\text{ref}})^2]$. Since the B frame is predicted by the L th enhancement layer of the reference frame, we have $\mathbb{E}[(v_i^{\text{ref}} - \widehat{v}_i^{\text{ref}})^2] = d_L$. Denoting by $d_i^{\text{ref}}(\mathbf{s}) = \mathbb{E}[(\epsilon_i^{\text{ref}})^2]$ the distortion of the reference frame, we have

$$\mathbb{E}[(\epsilon_i^{\text{dft}})^2] = d_i^{\text{ref}}(\mathbf{s}) - d_L. \quad (6)$$

Substituting (6) into (5), we have

$$d(\mathbf{s}) = d^{B^r}(z(\mathbf{s})) + \frac{1}{2} [d_1^{\text{ref}}(\mathbf{s}) + d_2^{\text{ref}}(\mathbf{s})] - d_L. \quad (7)$$

The distortion of the reference frame $d_i^{\text{ref}}(\mathbf{s})$ can be recursively estimated using (3) and (7). Because the prediction structure is acyclic, the recursion terminates when the reference frame is a key picture and (3) applies.

It should be noted that, in (7), the distortion is overestimated using an upper bound of (4), as will be shown by the simulation results in Section III-F. This overestimation does not sacrifice the quality of the decoded videos.

C. Finite-State Problem Formulation

Since the state space $\mathcal{V}^{\text{post}}$ is infinite, the state space \mathcal{S} is also infinite. Optimizing the scheduling policy over this infinite-state space is intractable. We define a set \mathcal{W}^{buf} as the data units in window \mathcal{W} and their associated predictors in \mathcal{W}^{pre} . With

³This assumption is empirically true. We calculated the correlation coefficient of $\widehat{v}_i^{\text{ref}} - v_i^{\text{ref}}$ and $v_i^{\text{ref}} - \widehat{v}_i^{\text{ref}}$ using the frames of test sequence *Foreman*, *Paris*, and *Bus*. The average correlation coefficient is 0.05.

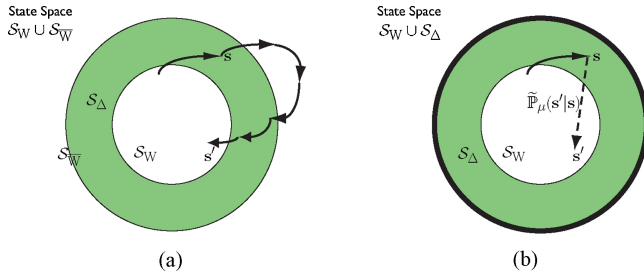


Fig. 6. Dynamics of the system Π_μ and the corresponding simplified system $\tilde{\Pi}_\mu$. (a) Π_μ . (b) $\tilde{\Pi}_\mu$.

Assumption 3, the scheduling policy is actually fixed when all the data in \mathcal{W}^{buf} are received. We only need to determine the optimal scheduling policy for states where some of the video data in \mathcal{W}^{buf} has not been received, which is a finite-state set. The system state, however, still evolves in the infinite-state space \mathcal{S} . In the following, we show how to simplify this infinite-state space problem to a finite-state problem.

We define the set of states where some of the video data in \mathcal{W}^{buf} has not been received as follows:

$$\mathcal{S}_W = \{\mathbf{s} | \mathbf{s} \in \mathcal{S}, \mathcal{W}^{\text{buf}} \not\subseteq \mathcal{O}(\mathbf{s})\} \quad (8)$$

where $\mathcal{O}(\mathbf{s})$ is the set of buffered video data units when the state is \mathbf{s} . We define another subset of \mathcal{S} as the complement of \mathcal{S}_W :

$$\mathcal{S}_{\bar{W}} = \{\mathbf{s} | \mathbf{s} \in \mathcal{S}, \mathcal{W}^{\text{buf}} \subseteq \mathcal{O}(\mathbf{s})\}. \quad (9)$$

For all the states in $\mathcal{S}_{\bar{W}}$, all the video data units in \mathcal{W}^{buf} has been received.

Given a policy $\mu(\cdot)$, the system state evolves as a controlled Markov chain in set $\mathcal{S}_W \cup \mathcal{S}_{\bar{W}}$. Because the transmission rate is finite, the number of states in $\mathcal{S}_{\bar{W}}$ that can be reached from \mathcal{S}_W in one step is also finite. We formally define this set of states as follows:

$$\mathcal{S}_\Delta = \{\mathbf{s}' | \mathbf{s}' \in \mathcal{S}_{\bar{W}}; \exists \mathbf{s} \in \mathcal{S}_W, \text{ s.t., } \mathbb{P}_\mu(\mathbf{s}' | \mathbf{s}) > 0\} \quad (10)$$

where $\mathbb{P}_\mu(\mathbf{s}' | \mathbf{s})$ is the state transition probability under policy μ (for the expression for $\mathbb{P}_\mu(\mathbf{s}' | \mathbf{s})$, see Appendix A). Thus, to move from \mathcal{S}_W into the set $\mathcal{S}_{\bar{W}}$, the system state first hits a state in \mathcal{S}_Δ and then stays in $\mathcal{S}_{\bar{W}}$ for some time. During this period, the decoded video distortion is always d_L , because all the layers in \mathcal{W}^{buf} are available. The evolution of the system when it moves into set $\mathcal{S}_{\bar{W}}$ affects the performance of the system. In general, the longer it stays in $\mathcal{S}_{\bar{W}}$, the better the performance is. Although the scheduling policy in $\mathcal{S}_{\bar{W}}$ is fixed as described in Assumption 3, the policy in \mathcal{S}_W determines how frequently the system state will hit $\mathcal{S}_{\bar{W}}$ and thus critically impacts the system performance.

In the following, we denote the system under a given policy μ as system Π_μ . Let $t_\mu(\mathbf{s})$ be the expected time spent by Π_μ in $\mathcal{S}_{\bar{W}}$ after it enters $\mathcal{S}_{\bar{W}}$ at state $\mathbf{s} \in \mathcal{S}_\Delta$. Let $\tilde{\mathbb{P}}_\mu(\mathbf{s}' | \mathbf{s})$ denote the probability that Π_μ jumps back to \mathcal{S}_W at state $\mathbf{s}' \in \mathcal{S}_W$ after it enters $\mathcal{S}_{\bar{W}}$ at state \mathbf{s} . To find the optimal policy, we define a finite-state system $\tilde{\Pi}_\mu$ as follows.

Definition 1: A system $\tilde{\Pi}_\mu$ is called the simplified system of the original system Π_μ if it has the following dynamics.

- 1) The system is a controlled semi-Markov process over state space $\tilde{\mathcal{S}} = \mathcal{S}_W \cup \mathcal{S}_\Delta$. In any state $\mathbf{s} \in \tilde{\mathcal{S}}$, the distortion is $d(\mathbf{s})$ as in (3) and (7). In any state in \mathcal{S}_W , the system evolves according to the policy μ . The system state transition probability is $\mathbb{P}_\mu(\cdot | \cdot)$.
- 2) When the system jumps to a state $\mathbf{s} \in \mathcal{S}_\Delta$, it spends $t_\mu(\mathbf{s})$ slots in \mathbf{s} with distortion d_L for each slot. The system then transitions to a state $\mathbf{s}' \in \mathcal{S}_W$ with probability $\tilde{\mathbb{P}}_\mu(\mathbf{s}' | \mathbf{s})$ (see Fig. 6).

It should be noted that $\tilde{\Pi}_\mu$ is not coupled with the original system Π_μ . It just shares some properties with the original system. The following theorem relates the distortion under $\tilde{\Pi}_\mu$ and that of Π_μ .

Theorem 1: If the jump chain of the original system Π_μ is positive recurrent, then the time-average video distortion of Π_μ is the same as the simplified system $\tilde{\Pi}_\mu$.

Proof Sketch: If the jump chain is positive recurrent, the jump from \mathcal{S}_W to \mathcal{S}_Δ can partition the Markov process into i.i.d. segments. We only need to optimize the policy μ to minimize the average distortion in each segment. Every segment consists of two consecutive subsegments. During the first subsegment, $\mathbf{s} \in \mathcal{S}_{\bar{W}}$. In the other subsegment, $\mathbf{s} \in \mathcal{S}_W$. Because every state in $\mathcal{S}_{\bar{W}}$ has the same distortion d_L , we can abstract the first subsegment as a single state with transition probability $\tilde{\mathbb{P}}_\mu(\cdot | \cdot)$. This simplified system provides the same average distortion as the original system. For a detailed proof, see the technical report [22]. ■

Remark 2: The positive recurrent condition for the jump chain means that the average throughput of the channel is neither too large nor too small relative to the average data rate of the video. If the average throughput of the channel is very large, the receiver buffer can always buffer enough frames and dynamic scheduling is unnecessary. If the average channel throughput is too small, the channel cannot support the video stream and dynamic scheduling cannot help either.

As indicated by Theorem 1, given any policy μ , the video distortion of Π_μ is the same as $\tilde{\Pi}_\mu$. Thus, we can optimize our policy with respect to $\tilde{\Pi}_\mu$, which has a finite-state space, and a standard policy optimization algorithm can be applied.

Before we can apply an MDP algorithm to optimize the policy, we need to compute $t_\mu(\mathbf{s})$ and $\tilde{\mathbb{P}}_\mu(\mathbf{s}' | \mathbf{s})$ for every state $\mathbf{s} \in \mathcal{S}_\Delta$ and $\mathbf{s}' \in \mathcal{S}_W$. Both $t_\mu(\mathbf{s})$ and $\tilde{\mathbb{P}}_\mu(\mathbf{s}' | \mathbf{s})$ only involve dynamics of the system in $\mathcal{S}_{\bar{W}}$. Details on how to compute $t_\mu(\mathbf{s})$ and $\tilde{\mathbb{P}}_\mu(\mathbf{s}' | \mathbf{s})$ are found in [22].

D. Determining Optimal Policy via Value Iteration

Given $t_\mu(\cdot)$ and $\tilde{\mathbb{P}}_\mu(\cdot | \cdot)$, the optimal policy for an MDP can be determined for the simplified system $\tilde{\Pi}_\mu$, which is also the optimal policy of Π_μ . Let \mathbf{s}^{ini} be any state in $\tilde{\mathcal{S}} = \mathcal{S}_W \cup \mathcal{S}_\Delta$. The hitting time to state \mathbf{s}^{ini} can partition the process into i.i.d. cycles. Optimizing the policy $\mu(\cdot)$ in the cycles minimizes the time-average video distortion of the system. Similar to the derivation in [23, p. 441], this is equivalent to an average-cost minimization problem with stage-cost $(d(\mathbf{s}) - \lambda) \eta(\mathbf{s})$, where λ is the expected average-cost of each cycle, i.e., the average

distortion. The function $\eta(\mathbf{s})$ is defined as

$$\eta(\mathbf{s}) = \begin{cases} 1 & : \mathbf{s} \in \mathcal{S}_W \\ t_\mu(\mathbf{s}) & : \mathbf{s} \in \mathcal{S}_\Delta. \end{cases}$$

Note that $d(\mathbf{s})$ is the cost of spending one slot on state \mathbf{s} and λ is the expected cost per slot. Therefore, $d(\mathbf{s}) - \lambda$ is the extra cost of spending one slot on state \mathbf{s} . Since $\eta(\mathbf{s})$ is the average time spent on state \mathbf{s} , $(d(\mathbf{s}) - \lambda)\eta(\mathbf{s})$ is the total extra cost of visiting state \mathbf{s} . Let us denote by $h(\mathbf{s})$ the average cost to go in each cycle when the system starts at state \mathbf{s} . Then, we have the following Bellman's equation array:

$$h(\mathbf{s}) = (d(\mathbf{s}) - \lambda)\eta(\mathbf{s}) + \sum_{\mathbf{s}' \in \mathcal{S}_W \cup \mathcal{S}_\Delta} \mathbb{P}_\mu(\mathbf{s}'|\mathbf{s})h(\mathbf{s}') \quad (11)$$

where $h(\mathbf{s}^{\text{ini}}) = 0$. To find the optimal policy, the standard value iteration algorithm can be applied [23, p. 430].

On the one hand, the assumptions on scheduling policy result in the finite-state MDP-based formulation. On the other hand, the assumptions may render the derived scheduling policy suboptimal. To verify that the performance of the scheduling policy derived from the MDP formulation is actually close to optimal, we prove a performance upper bound in the next section.

E. Performance Upper Bound

As discussed in Section II-C, $\{d^k(z_t), k \in \mathcal{K}\}$ are the rate quality models of type- k frames when all the predictors have also been received. Since $d^k(z_t)$ does not incorporate the distortion due to drift, the time-average distortion of the transmitted video is at least $\frac{1}{n} \sum_{t=1}^n \sum_{k \in \mathcal{K}} d^k(z_t) \mathbb{1}_t^k$, where n is the number of frames in the video sequence and $\mathbb{1}_t^k$ is the indicator that the t th frame is a type- k frame. Let r_t be the amount of data that is received in the t th slot; a distortion lower bound of any scheduler is given by the following offline optimization problem

$$\begin{aligned} & \underset{z_{1:n}}{\text{minimize}} && \frac{1}{n} \sum_{k \in \mathcal{K}} \sum_{t=1}^n d^k(z_t) \mathbb{1}_t^k \\ & \text{s.t.} && \frac{1}{t} \sum_{i=1}^t z_i \leq \frac{1}{t} \sum_{i=1}^t r_i, \quad \forall t \in \{1, 2, \dots, n\} \end{aligned} \quad (12)$$

where the constraint $\frac{1}{t} \sum_{i=1}^t z_i \leq \frac{1}{t} \sum_{i=1}^t r_i$ guarantees that the received data for the frames displayed before time t does not exceed the cumulative throughput prior to time t . We can further relax the constraints in (12) by only keeping the last one, i.e., when $t = n$. The relaxed optimization problem is then given by

$$\begin{aligned} & \underset{z_{1:n}}{\text{minimize}} && \frac{1}{n} \sum_{k \in \mathcal{K}} \sum_{t=1}^n d^k(z_t) \mathbb{1}_t^k \\ & \text{s.t.} && \frac{1}{n} \sum_{t=1}^n z_t \leq \frac{1}{n} \sum_{t=1}^n r_t. \end{aligned} \quad (13)$$

Let $\widehat{d}^k(z_t)$ be the convex envelope of $d^k(z_t)$ (see Fig. 4). Since $d^k(z_t)$ are lower bounded by $\widehat{d}^k(z_t)$, we can bound

problem (13) by

$$\begin{aligned} & \underset{z_{1:n}}{\text{minimize}} && \frac{1}{n} \sum_{k \in \mathcal{K}} \sum_{t=1}^n \widehat{d}^k(z_t) \mathbb{1}_t^k \\ & \text{s.t.} && \frac{1}{n} \sum_{t=1}^n z_t \leq \frac{1}{n} \sum_{t=1}^n r_t. \end{aligned} \quad (14)$$

Let $n^k = \sum_{t=1}^n \mathbb{1}_t^k$ denotes the number of type- k frames. Since the functions $\widehat{d}^k(z_t)$ are convex, by Jensen's inequality, we have

$$\frac{1}{n^k} \sum_{t=1}^n \widehat{d}^k(z_t) \mathbb{1}_t^k \geq \widehat{d}^k \left(\frac{1}{n^k} \sum_{t=1}^n z_t \mathbb{1}_t^k \right).$$

Problem (14) can then be bounded by

$$\begin{aligned} & \underset{z_{1:n}}{\text{minimize}} && \sum_{k \in \mathcal{K}} \frac{n^k}{n} \widehat{d}^k \left(\frac{1}{n^k} \sum_{t=1}^n z_t \mathbb{1}_t^k \right) \\ & \text{s.t.} && \sum_{k \in \mathcal{K}} \frac{n^k}{n} \left(\frac{1}{n^k} \sum_{t=1}^n z_t \mathbb{1}_t^k \right) \leq \frac{1}{n} \sum_{t=1}^n r_t. \end{aligned} \quad (15)$$

If the video is reasonably long, e.g., several minutes, the frame number n will be very large. If we let $n \rightarrow \infty$ and assume the channel throughput r_t is ergodic, $\frac{1}{n} \sum_{t=1}^n r_t$ will converge to the ergodic capacity $r^{\text{avg}} = \lim_{n \rightarrow \infty} \frac{1}{n} \sum_{t=1}^n r_t$. Furthermore, let F^k denote the number of type- k frames in an intraperiod. We have $\frac{n^k}{n} \rightarrow \frac{F^k}{F^{\text{intra}}}$. Similarly, for stationary policies,⁴ the limits $z^k = \lim_{n \rightarrow \infty} \frac{1}{n^k} \sum_{t=1}^n z_t \mathbb{1}_t^k$ exist. We have $\lim_{n \rightarrow \infty} \left[\frac{n^k}{n} \left(\frac{1}{n^k} \sum_{t=1}^n z_t \mathbb{1}_t^k \right) \right] = \frac{F^k}{F^{\text{intra}}} z^k$. Thus, we have shown the following theorem.

Theorem 2: For ergodic wireless throughput and stationary adaptive scheduling policies, the following optimization gives an upper bound on performance (lower bound of distortion):

$$\begin{aligned} & \underset{z^k, k \in \mathcal{K}}{\text{minimize}} && \sum_{k \in \mathcal{K}} \frac{F^k}{F^{\text{intra}}} \widehat{d}^k(z^k) \\ & \text{s.t.} && \sum_{k \in \mathcal{K}} \frac{F^k}{F^{\text{intra}}} z^k \leq r^{\text{avg}}. \end{aligned} \quad (16)$$

Since the rate-distortion function $\widehat{d}^k(\cdot)$ is assumed to be convex, the above optimization problem is convex and easily solved. In Section III-F, this performance bound will be employed as a benchmark to evaluate the performance of our MDP-based scheduling policy.

F. Performance Evaluation of the MDP-Based Scheduling Policy

In this section, we evaluate the performance of the policy obtained from our MDP-based formulation. The algorithm was evaluated on test sequences *Foreman*, *Bus*, *Flower*, *Mobile*, and *Paris* [24]. These video sequences were encoded using H.264/SVC reference software JSVM [25] with a base layer and a CGS enhancement layers. The intraperiod and IDR period were set to $F^{\text{intra}} = 16$. The GOP length was fixed at $F^{\text{GOP}} = 4$. The QP of the base layer, denoted by QP^{base} ,

⁴A policy is called stationary if it is a function of state \mathbf{s} and the function is invariant with respect to time t .

TABLE I
ENCODING PARAMETERS AND RATE-DISTORTION MODEL PARAMETERS OF THE TESTED SEQUENCES

Sequences	Layer 0 (base layer)			Layer 1			Layer 2		
	QP	$\omega_0^I, \omega_0^P, \omega_0^{B^1}, \omega_0^{B^2}$ /Byte	d_0 /MSE	$\omega_1^I, \omega_1^P, \omega_1^{B^1}, \omega_1^{B^2}$ /Byte	d_1 /MSE	$\omega_2^I, \omega_2^P, \omega_2^{B^1}, \omega_2^{B^2}$ /Byte	d_2 /MSE		
<i>Foreman</i>	30	6712, 2499, 928, 520	16.27	8302, 8293, 3373, 2775	5.491	5844, 5773, 2177, 1893	4.124		
<i>Bus</i>	38	5920, 2417, 889, 568	100.8	7837, 8003, 3390, 2925	41.35	4636, 4412, 1577, 1339	21.65		
<i>Flower</i>	40	8261, 2076, 548, 324	172.1	6786, 6900, 1951, 1611	96.66	6633, 6610, 2008, 1545	30.85		
<i>Mobile</i>	40	9648, 1556, 510, 262	186.0	9090, 9193, 2541, 2171	89.90	7627, 6894, 1973, 1701	37.35		
<i>Paris</i>	32	12353, 2640, 865, 463	32.33	9850, 9457, 2103, 1571	18.59	8091, 7987, 2024, 1555	5.420		

was chosen such that the data rate of the base layer is lower than the average channel throughput. The QP of the CGS enhancement layer is set as $QP^{\text{base}} - 10$. We employ this configuration to make sure that the channel is at least good enough to support the base layer. Otherwise, any scheduling policy cannot provide acceptable video quality. The CGS is split into two MGS layers. The first MGS layer contains six of the 16 transform coefficients of the CGS layer. The other ten coefficient belongs to the second MGS layer. The QPs and rate-distortion model parameters of the encoded video sequences are shown in Table I. Parallel to [9] and [10], we employ the FSMC channel model proposed in [17] to model the dynamics of Rayleigh fading channels. The SNR at the receiver is partitioned into four regions using the algorithm proposed in [17]. In our simulations, we set the average SNR to $\Lambda^{\text{avg}} = 10\text{dB}$. For each sequence, 200 transmissions were sent over the simulated channel. A startup delay constraint was fixed to 200 ms, i.e., video playback began six frames after the transmission began. After each transmission, a trace file that recorded the packet loss in each time slot was generated. We used the bitstream extractor of JSVM to remove those dropped packets. The extracted bitstreams were decoded using the JSVM decoder with frame copy error concealment. For more details about the FSMC channel model, see Appendix B.

The performance of the MDP-based scheduling algorithm was tested over the simulated Markov channel models with different Doppler frequencies ($f^d = 5$ and 3Hz, respectively). The simulation results are summarized in Tables II and III. The visual quality is measured via the MS-SSIM index that correlates well with human objective judgments [26]. The time-averaged MS-SSIM value is further converted to difference mean opinion score (DMOS) using the following mapping

$$q^{\text{dmos}} = 13.3442 \log(1 - q^{\text{ssim}}) + 3.6226(1 - q^{\text{ssim}}) + 77.0117 \quad (17)$$

where q^{ssim} denotes the time-averaged quality measured in MS-SSIM and q^{dmos} is the corresponding DMOS value. Equation (17) is obtained by logistic regression using the MS-SSIM indices and MOS values of the images in the LIVE database [27]. DMOS ranges from 0 to 100. Value 0 means perfect visual quality and value 100 means bad visual quality. Roughly speaking, value 50 means fair quality. It can be seen from Tables II and III that the DMOS value of the MDP-based scheduling policy is worse than the performance bound by at most 2, which is visually insignificant. Given that the bound given by Theorem 2 is an upper bound (i.e., a lower bound

of DMOS value), the MDP-based scheduling policy is indeed near-optimal.

IV. NEAR-OPTIMAL HEURISTIC ONLINE SCHEDULING ALGORITHM

Although the MDP-based formulation makes it possible to compute a good scheduling policy using value iteration algorithm, offline computation of such policies requires *a priori* knowledge of the channel dynamics. This motivates us to design a simple online scheduling policy that delivers similar performance as the MDP-based policy that only requires little *a priori* knowledge about the channel dynamics.

A good online video scheduling algorithm should explicitly take advantage of the channel dynamics and schedule data from different quality layers as a function of the receiver buffer state. There are three fundamental questions in designing such a scheduler: 1) How should one incorporate limited knowledge of channel dynamics in adaptive scheduling? 2) How should one determine the number of enhancement layers to schedule? 3) How should one allocate appropriate transmission rate among current and future intraperiods. In the following, we will show how to address these fundamental problems by reasonably simplifying the MDP-based scheduling algorithm.

A. Channel Model Simplification

In a practical wireless communication environment, accurate channel dynamics models such as the state transition probability \mathbf{P}^c are not generally available. Some basic characteristics for the channel dynamics can, however, be easily used. At any slot t , the instantaneous channel throughput r_t can be estimated using receiver channel state information as

$$\hat{r}_t = x_t(1 - y_t),$$

where (x_t, y_t) is the channel state at t (see Section III-A). The ergodic channel throughput r^{avg} can be estimated by averaging \hat{r}_t over time. If we model r_t as the realization of a random process $\{R_t, t \in \mathbb{N}\}$, the temporal correlation coefficient $\rho = \frac{\text{cov}(R_t, R_{t+1})}{\sigma(R_t)\sigma(R_{t+1})}$ can also be estimated from \hat{r}_t . Further, it is reasonable to assume the channel throughput R_t will typically regress to the mean r^{avg} . This inspires us to use a simple autoregressive model to capture the dynamics of the channel. A first order autoregressive model [AR(1)] for R_t is given as

$$R_t - \phi R_{t-1} = c + N_t \quad (18)$$

TABLE II

PERFORMANCE OF THE NEAR-OPTIMAL POLICY IN SSIM-PREDICTED DMOS, $f^d = 5$

	<i>Paris</i>	<i>Mobile</i>	<i>Flower</i>	<i>Bus</i>	<i>Foreman</i>
MDP Policy	26.9020	38.9033	34.5826	41.8721	32.2426
Upper bound	25.6017	38.0842	34.0626	41.4600	31.6807

TABLE III

PERFORMANCE OF THE NEAR-OPTIMAL POLICY IN SSIM-PREDICTED DMOS, $f^d = 3$

	<i>Paris</i>	<i>Mobile</i>	<i>Flower</i>	<i>Bus</i>	<i>Foreman</i>
MDP Policy	27.1376	39.0452	35.7828	42.0808	32.4431
Upper bound	25.2314	37.9431	33.7052	41.2611	31.4852

where N_t is an i.i.d. random variable with zero-mean value. From (18), parameter c and ϕ can be estimated as $\phi = \rho$ and $c = r^{\text{avg}}(1 - \rho)$ [28, p. 115]. Thus, we have

$$R_t - \rho R_{t-1} = r^{\text{avg}}(1 - \rho) + N_t. \quad (19)$$

Using this autoregressive model, the amount of data that will be delivered in the next ζ slots by the channel can be estimated as

$$g(\hat{r}_t) = \mathbb{E} \left[\sum_{a=0}^{\zeta-1} R_{t+a} | R_t = \hat{r}_t \right] = \sum_{a=0}^{\zeta-1} [\hat{r}_t \rho^a + r^{\text{avg}}(1 - \rho^a)]. \quad (20)$$

To obtain an accurate estimate in the near future, we set the length of the window ζ into the future that will be considered to be the relaxation time⁵ of the channel, i.e., $\zeta = \lceil -(\ln \rho)^{-1} \rceil$. In the following, we use this to determine which quality layers to schedule.

B. Layer Selection

Given the current channel state, receiver buffer state, and estimated available capacity for a window ζ into the future, the goal is to determine which layers to schedule. We will focus on determining the number of enhancement layers which should be scheduled. We denote by $L^{\text{sch}}(\mathbf{s}_t)$ the number of layers to be scheduled if the state is \mathbf{s}_t . Once $L^{\text{sch}}(\mathbf{s}_t)$ is determined, the online scheduling algorithm only schedules data units from the first $L^{\text{sch}}(\mathbf{s}_t)$ layers.

The layer selection scheme for our proposed online algorithm is motivated by that of the MDP-based policy. Using $g(\hat{r}_t)$ defined in (20), we can estimate the amount of data that can be delivered in the next ζ slots. Let $\Gamma(\ell, \mathbf{s}_t)$ be the amount of data that is not currently available at the playback buffer at time t , and belongs to the first ℓ layers of the next ζ frames that have not been decoded. The quantities $g(\hat{r}_t)$ and $\Gamma(\ell, \mathbf{s}_t)$ summarize the channel and buffer states for the next ζ slots. Note that $\Gamma(\ell - 1, \mathbf{s}_t) \leq g(\hat{r}_t) < \Gamma(\ell, \mathbf{s}_t)$ means that we can probably transmit all the data up to the ℓ th layer in the next ζ slots. Intuitively, we can simply choose $L^{\text{sch}}(\mathbf{s}_t) = \ell - 1$ when $\Gamma(\ell - 1, \mathbf{s}_t) \leq g(\hat{r}_t) < \Gamma(\ell, \mathbf{s}_t)$. As discussed next, this

⁵The relaxation time is defined as the temporal distance at which the temporal correlation coefficient is reduced to $\frac{1}{2}$.

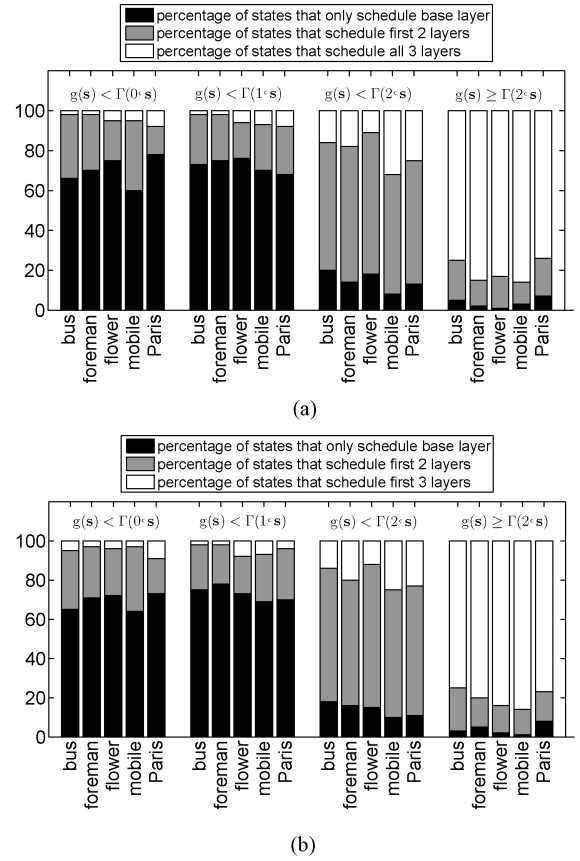


Fig. 7. Given different relationship between $g(\mathbf{s})$ and $\Gamma(\ell, \mathbf{s})$, the proportions of states corresponding to different $L^{\text{sch}}(\mathbf{s})$ are shown in different colors. Results are obtained under Rayleigh fading channels with different Doppler shifts and are calculated on five different video sequences (*Bus*, *Foreman*, *Flower*, *Mobile*, and *Paris*). (a) $f^d = 5$ Hz. (b) $f^d = 3$ Hz.

layer selection scheme can be motivated by the near-optimal scheduling policies computed for the MDP-based model.

Note that $\hat{r}_t = x_t(1 - y_t)$ is determined by state \mathbf{s}_t ; thus, $g(\hat{r}_t)$ can also be written as a function of \mathbf{s}_t , i.e., $g(\mathbf{s}_t)$. Suppose we partition the state space into subsets $\mathcal{P}^\ell = \{\mathbf{s} \in \mathcal{S} : \Gamma(\ell - 1, \mathbf{s}) \leq g(\mathbf{s}) < \Gamma(\ell, \mathbf{s})\}$, $\ell \in \{1, \dots, L + 2\}$ and calculate the fraction of states in \mathcal{P}^ℓ where the MDP-based policy only schedules the first $\ell - 1$ layers.⁶ As shown in Fig. 7, for 71% of the states of \mathcal{P}^1 and \mathcal{P}^2 , the MDP-based policy only schedules the first layer. For about 65% of the states of \mathcal{P}^3 , the MDP-based policy only schedules the first two layers. Finally, the MDP-based policy will schedule all the layers on 81% of the states in \mathcal{P}^4 . These observations justify our intuition regarding layer selection. In our proposed online scheduling algorithm, we will simply choose $L^{\text{sch}}(\mathbf{s}_t) = \ell - 1$ if $\Gamma(\ell - 1, \mathbf{s}_t) \leq g(\mathbf{s}_t) < \Gamma(\ell, \mathbf{s}_t)$. In other words, our heuristic algorithm determines $L^{\text{sch}}(\mathbf{s}_t)$ by roughly estimating the number of layers that can be transmitted.

C. Resource Allocation Between Current and Future Intra-periods

In each transmission slot, about \hat{r}_t bits of video data are delivered to the receiver. In the following, we refer to \hat{r}_t as

⁶We define $\Gamma(L + 2, \mathbf{s}_t) = +\infty$.

Algorithm 1 Online Adaptive Scheduling Algorithm**Input:** \mathbf{s}_t , r^{avg} , x_t , y_t , and ρ

```

1:  $\zeta = \lceil -(\ln \rho)^{-1} \rceil$ ;  $\hat{r}_t = x_t(1 - y_t)$ 
2: loop  $t$ 
3:    $g(\hat{r}_t) \leftarrow \sum_{a=0}^{\zeta-1} [\hat{r}_t \rho^a + r^{\text{avg}}(1 - \rho^a)]$ 
4:   for  $\ell = 1 \rightarrow L + 1$  do
5:     Compute  $\Gamma(\ell, \mathbf{s}_t)$ 
6:     if  $g(\hat{r}_t) < \Gamma(\ell, \mathbf{s}_t)$ 
7:       break
8:     end if
9:   end for
10:  if  $\ell = 1$  then
11:     $L^{\text{sch}}(\mathbf{s}_t) \leftarrow 1$ 
12:  else
13:     $L^{\text{sch}}(\mathbf{s}_t) \leftarrow \ell - 1$ 
14:  end if
15:  Compute  $\Psi^{\text{cur}}(L^{\text{sch}}, \mathbf{s}_t)$  and  $\Psi^{\text{l}}(L^{\text{sch}}, \mathbf{s}_t)$ 
16:   $\Omega_t \leftarrow \frac{\Psi^{\text{l}}(L^{\text{sch}}, \mathbf{s}_t)}{\Psi^{\text{cur}}(L^{\text{sch}}, \mathbf{s}_t) + \Psi^{\text{l}}(L^{\text{sch}}, \mathbf{s}_t)}$ 
17:  Schedule  $\min(\Omega_t \times \hat{r}_t, \Psi^{\text{l}}(L^{\text{sch}}, \mathbf{s}_t))$  bits from  $\mathcal{I}$ .
18:  Schedule  $\hat{r}_t - \min(\Omega_t \times \hat{r}_t, \Psi^{\text{l}}(L^{\text{sch}}, \mathbf{s}_t))$  bits from other
    active frames.
19: end loop

```

the budget for slot t . Once $L^{\text{sch}}(\mathbf{s}_t)$ is determined, we still need to determine how to allocate this budget among current and future intraperiods. Sometimes it is necessary to transmit data associated with next I frame before the data units in the current intraperiod. For example, when the next I frame is approaching its display deadline and its base layer has not yet been received, if we focus on transmitting the frames in the current intraperiod sequentially, this increases the risk that the next I frame cannot be decoded before its deadline. This in turn would cause severe decoding failures throughout the next intraperiod.

Let \mathcal{I} be the data units in the undecoded I frame that has the earliest display deadline. We denote by $\Psi^{\text{cur}}(\ell, \mathbf{s}_t)$ the amount of unreceived data in the first ℓ th layer of current intraperiod at state \mathbf{s}_t . We denote by $\Psi^{\text{l}}(\ell, \mathbf{s}_t)$ the amount of unreceived data in the first ℓ th layer of \mathcal{I} at state \mathbf{s}_t . We propose the following heuristic for allocating the bit budget between current intraperiod and \mathcal{I} . In each transmission slot, the scheduling algorithm allocates up to $\Omega_t = \frac{\Psi^{\text{l}}(L^{\text{sch}}(\mathbf{s}_t), \mathbf{s}_t)}{\Psi^{\text{cur}}(L^{\text{sch}}(\mathbf{s}_t), \mathbf{s}_t) + \Psi^{\text{l}}(L^{\text{sch}}(\mathbf{s}_t), \mathbf{s}_t)}$ of the transmission bit budget to \mathcal{I} . In other words, the number of bits allocated to \mathcal{I} is $\min(\Omega_t \times \hat{r}_t, \Psi^{\text{l}}(L^{\text{sch}}(\mathbf{s}_t), \mathbf{s}_t))$.

Here, Ω_t gives the relative importance of the next I frame and current intraperiod. If $\Psi^{\text{l}}(L^{\text{sch}}(\mathbf{s}_t), \mathbf{s}_t) = 0$, then $\Omega_t = 0\%$. It is not necessary to transmit any data for the next I frame. If $\Psi^{\text{cur}}(L^{\text{sch}}(\mathbf{s}_t), \mathbf{s}_t) = 0$, then $\Omega_t = 100\%$. We only focus on transmitting the future intraperiods.

The online scheduling algorithm is summarized in Algorithm 1.

D. Performance Evaluation of the Online Scheduling Algorithm

The performance of the online scheduling algorithm was tested over the simulated Markov channel models with differ-

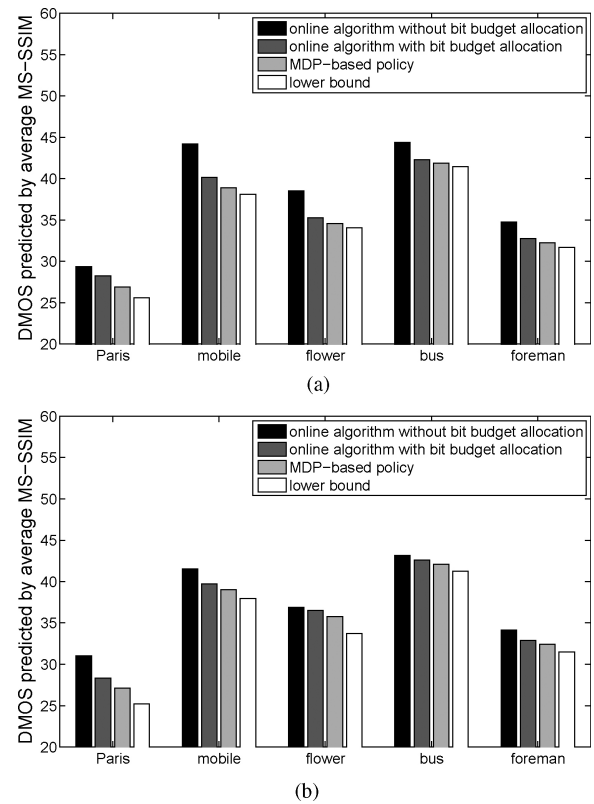


Fig. 8. Performance comparison of different scheduling algorithms. Video quality is measured in DMOS which is predicted by MS-SSIM using (17). (a) $f^d = 5$ Hz. (b) $f^d = 3$ Hz.

ent Doppler frequencies ($f^d = 5$ and 3 Hz, respectively). This setting is the same as the simulation setting in Section III-F. The results are summarized in Fig. 8. As can be seen, the performance of the proposed online scheduling algorithm is almost as good as the MDP-based scheduling algorithm. Moreover, the online scheduling algorithm's performance is close to the bound given by Theorem 2. We conclude it is a near-optimal scheduling algorithm.

We have also tested the performance of the online algorithm without bit budget allocation between current and future intraperiods. As can be seen, the performance is worse than the MDP-based scheduling policy and the performance bound. This motivates the necessity of allocating bit between current and future intraperiods.

V. CONCLUSION

We developed adaptive scheduling algorithms for stored scalable video transmission in wireless channels. By modeling the wireless channel as a Markov chain, an MDP model was proposed in which policies that minimize the distortion of decoded videos can be computed. By simplifying the scheduling algorithm obtained from the MDP formulation, we proposed an online scheduling algorithm that only requires limited knowledge of channel dynamics. Simulation results demonstrated the near-optimality of the proposed online scheduling policy versus a proposed bound on performance.

APPENDIX A
TRANSITION PROBABILITY

Notations: Let $\mathbf{1}$ be the unit vector of all-ones and $\mathbf{0}$ be the zero vector. $\max\{\mathbf{a}, \mathbf{b}\}$ is the componentwise maximum of vector \mathbf{a} and \mathbf{b} . $\mathbb{1}(\cdot)$ is the indicator function.

Let $\mathbf{s}_t = (\mathbf{c}_t, \mathbf{v}_t)$ and \mathcal{U}_s be the system state and the corresponding feasible control set at slot t , where $\mathbf{c}_t = (x_t, y_t)$ and $\mathbf{v}_t = (v_t^I, \mathbf{v}_t^{\text{pre}}, \mathbf{v}_t^{\text{W}}, \mathbf{v}_t^{\text{post}})$. At the beginning of each slot, one frame is decoded and played out. Let $\mathbf{v}_t^+ = (v_t^{I+}, \mathbf{v}_t^{\text{pre}+}, \mathbf{v}_t^{\text{W}+}, \mathbf{v}_t^{\text{post}+})$ denote the buffer state right after the first frame is displayed. For \mathbf{v}_t^{I+} , we have

$$\mathbf{v}_t^{I+} = \begin{cases} F^{\text{intra}} - 1 & \text{if } v_t^I = 0 \\ v_t^I - 1 & \text{if } v_t^I \neq 0. \end{cases} \quad (21)$$

The first frame in \mathcal{W} is moved into \mathcal{W}^{pre} ; thus, we have

$$\mathbf{v}_t^{\text{pre}+} = (b_{f_{\text{key}}}^{\text{pre}}, \dots, b_{-1}^{\text{pre}}, b_0^{\text{W}}). \quad (22)$$

The first frame in $\mathcal{W}^{\text{post}}$ moves into \mathcal{W} . Thus, we have

$$\mathbf{v}_t^{\text{W}+} = (\mathbf{b}_1^{\text{W}}, \dots, \mathbf{b}_{L-1}^{\text{W}}, \sum_{\ell=0}^L \mathbb{1}(\mathbf{b}_\ell^{\text{post}} \geq \mathbf{1})). \quad (23)$$

For the set $\mathcal{W}^{\text{post}}$, once the current frame is played out, we have

$$\mathbf{v}_t^{\text{post}+} = \max\{\mathbf{v}_t^{\text{post}} - \mathbf{1}, \mathbf{0}\}. \quad (24)$$

After the first frame is displayed, the transmitter begins to sequentially transmit the collection of video data units indicated by the action $\mathcal{U}_t = \mu(\mathbf{s}_t) = \{(f_1, \ell_1), \dots, (f_{|\mathcal{U}_t|}, \ell_{|\mathcal{U}_t|})\}$. Let $\Delta\mathcal{U}_t = \{(f_1, \ell_1), \dots, (f_{n_t}, \ell_{n_t})\}$ denote the completely received data units by the end of the slot, where n_t is the number of received data units. Among the data units in $\Delta\mathcal{U}_t$, let $\Delta\mathbf{v}_t^{\text{pre}}$ and $\Delta\mathbf{v}_t^{\text{W}}$ be the number of newly received data units for each frame in set $\mathcal{W}^{\text{pre}+}$ and $\mathcal{W}^{\text{W}+}$, respectively. At the beginning of the $(t+1)$ th slot, we have the following state transition relationship:

$$\mathbf{v}_{t+1}^{\text{pre}} = \mathbf{v}_t^{\text{pre}+} + \Delta\mathbf{v}_t^{\text{pre}} \quad (25)$$

$$\mathbf{v}_{t+1}^{\text{W}} = \mathbf{v}_t^{\text{W}+} + \Delta\mathbf{v}_t^{\text{W}}. \quad (26)$$

Similarly, we denote by $\Delta\mathbf{v}_t^{\text{post}} = (\Delta b_0^{\text{post}}, \dots, \Delta b_L^{\text{post}})$ the number of newly received data units for each layer in frame set $\mathcal{W}^{\text{post}+}$. The state transition relationship of $\mathcal{W}^{\text{post}}$ is

$$\mathbf{v}_{t+1}^{\text{post}} = \mathbf{v}_t^{\text{post}+} + \Delta\mathbf{v}_t^{\text{post}}. \quad (27)$$

The amount of video data in $\Delta\mathcal{U}_t$, denoted by $\Phi(\mathbf{v}_t, \Delta\mathcal{U}_t)$, can be estimated according to buffer state v_t^I and the rate-quality model introduced in Section II-C. Specifically, for each data unit in $\Delta\mathcal{U}_t$, we first determine the frame type according to v_t^I and then estimate the amount of data by the rate-quality model. The set $\Delta\mathcal{U}_t$ records the completely transmitted data units up to (f_{n_t}, ℓ_{n_t}) th data unit. However, data unit $(f_{n_t+1}, \ell_{n_t+1})$ is only partially received. Denoting the amount of data in unit $(f_{n_t+1}, \ell_{n_t+1})$ by $\tilde{\Phi}(\mathbf{v}_t^I, \Delta\mathcal{U}_t)$, the amount of received data is at least $\Phi(\mathbf{v}_t^I, \Delta\mathcal{U}_t)$ and at most $\Phi(\mathbf{v}_t^I, \Delta\mathcal{U}_t) + \tilde{\Phi}(\mathbf{v}_t^I, \Delta\mathcal{U}_t)$. Assuming the physical layer packet length is L^{PHY} , there is $N = \lceil \frac{x_t}{L^{\text{PHY}}} \rceil$ packet transmissions during a time slot.

The number of successfully transmitted packets is at least $N_l = \lceil \frac{\Phi(\mathbf{v}_t^I, \Delta\mathcal{U}_t)}{L^{\text{PHY}}} \rceil$ and is less than $N_h = \lceil \frac{\Phi(\mathbf{v}_t^I, \Delta\mathcal{U}_t) + \tilde{\Phi}(\mathbf{v}_t^I, \Delta\mathcal{U}_t)}{L^{\text{PHY}}} \rceil$. As assumed in Section II-D, the channel state is constant over each slot. Thus, the packet losses are independent within each slot. The number of successful packet transmissions in a slot is distributed binomially. Hence, the state transition probability from $\mathbf{s}_t = (\mathbf{c}_t, \mathbf{v}_t)$ to $\mathbf{s}_{t+1} = (\mathbf{c}_{t+1}, \mathbf{v}_{t+1})$ is

$$\mathbb{P}_\mu(\mathbf{s}_{t+1}|\mathbf{s}_t) = \left[\sum_{n_t=N_l}^{N_h-1} \binom{N}{n_t} y_t^{N-n_t} (1-y_t)^{n_t} \right] \mathbb{P}(\mathbf{c}_{t+1}|\mathbf{c}_t) \quad (28)$$

where the first multiplicative term is the transition probability of the receiver buffer state from \mathbf{v}_t to \mathbf{v}_{t+1} and the second term is the transition probability of the channel state from \mathbf{c}_t to \mathbf{c}_{t+1} .

APPENDIX B
SIMULATION SETTINGS

We employ the FSMC channel model proposed in [17] to model the dynamics of Rayleigh fading channels. The SNR at the receiver is partitioned into $|\mathcal{C}|$ regions using the algorithm proposed in [17]. Let Λ_i be the partition thresholds, where $\Lambda_0 = -\infty$ and $\Lambda_{|\mathcal{C}|} = \infty$. Let $\tilde{\Lambda}_k$ be the representative SNR in the k th region. For Rayleigh fading channels, we have

$$\tilde{\Lambda}_k = \frac{\int_{\Lambda_{k-1}}^{\Lambda_k} \lambda p(\lambda) d\lambda}{\int_{\Lambda_{k-1}}^{\Lambda_k} p(\lambda) d\lambda} \quad (29)$$

where $p(\lambda) = \frac{1}{\Lambda^{\text{avg}}} \exp(-\frac{\lambda}{\Lambda^{\text{avg}}})$ is the probability distribution function of the received instantaneous SNR of Rayleigh fading channels with average SNR Λ^{avg} . According to [17], the state transition probability \mathbf{P}^c is computed as

$$\mathbf{P}_{i,j}^c = \begin{cases} \frac{\mathcal{K}(\Lambda_j)\Delta T}{\pi_i}, & \text{if } j = i + 1 \\ \frac{\mathcal{K}(\Lambda_i)\Delta T}{\pi_i}, & \text{if } j = i - 1 \\ 1 - \frac{\mathcal{K}(\Lambda_j)\Delta T}{\pi_i} - \frac{\mathcal{K}(\Lambda_i)\Delta T}{\pi_i}, & \text{if } j = i \\ 0, & \text{otherwise} \end{cases} \quad (30)$$

where $\pi_i = \int_{\Lambda_{i-1}}^{\Lambda_i} p(\lambda) d\lambda$. $\mathcal{K}(\Lambda_i) = \sqrt{\frac{2\pi\Lambda_i}{\Lambda^{\text{avg}}}} f^d \exp(-\frac{\Lambda_i}{\Lambda^{\text{avg}}})$ is the level crossing rate of threshold Λ_i where f^d is the Doppler frequency. The coherence time is estimated via $t_{\text{cor}} = 0.423/f^d$. In our simulations, we set $|\mathcal{C}| = 4$ and $\Lambda^{\text{avg}} = 10\text{dB}$.

We assume that BPSK, QPSK, and 8PSK are used for modulation. The symbol error rate p_k^s in the k th SNR region is $p_k^s = 2Q(\sqrt{2\tilde{\Lambda}_k} \sin \frac{\pi}{2M})$, where $M = 1, 2, 3$ for BPSK, QPSK, and 8PSK, respectively. Each packet contains 2048 symbols. Thus, the packet length $L^{\text{PHY}} = 2048 \times M$, where $M = 1, 2$, and 3 for BPSK, QPSK, and 8PSK, respectively. The transmission time for each packet is $\Delta t = 1.5$ ms. The transmission data rate is given by $x_k = \frac{\Delta T}{\Delta t} L^{\text{PHY}}$. The packet error rate is given by $y_k = 1 - (1 - p_k^s)^{2048}$. The modulation scheme for k th channel states is chosen such that the throughput $x_k(1 - y_k)$ is maximized.

REFERENCES

- [1] H. Schwarz, D. Marpe, and T. Wiegand, "Overview of the scalable video coding extension of the H.264/AVC standard," *IEEE Trans. Circuits Syst. Video Technol.*, vol. 17, no. 9, pp. 1103–1120, Sep. 2007.

- [2] W. Li, "Overview of fine granularity scalability in MPEG-4 video standard," *IEEE Trans. Circuits Syst. Video Technol.*, vol. 11, no. 3, pp. 301–317, Mar. 2001.
- [3] M. Podolsky, S. McCanne, and M. Vetterli, "Soft ARQ for layered streaming media," Div. Comput. Sci., Univ. Calif., Berkeley, Tech. Rep. UCB/CSD-98-1024, 1998.
- [4] P. de Cuetos and K. W. Ross, "Optimal streaming of layered video: Joint scheduling and error concealment," in *Proc. Int. Conf. Multimedia*, 2003, pp. 55–64.
- [5] P. A. Chou and Z. Miao, "Rate-distortion optimized streaming of packetized media," *IEEE Trans. Multimedia*, vol. 8, no. 2, pp. 390–404, Apr. 2006.
- [6] J. Chakareski, P. A. Chou, and B. Aazhang, "Computing rate-distortion optimized policies for streaming media to wireless clients," in *Proc. Data Compress. Conf.*, 2002, pp. 53–62.
- [7] N. Changuel, N. Mastrorade, M. Van der Schaar, B. Sayadi, and M. Kieffer, "End-to-end stochastic scheduling of scalable video overtime-varying channels," in *Proc. Int. Conf. Multimedia*, 2010, pp. 731–734.
- [8] F. Fu and M. van der Schaar, "A new systematic framework for autonomous cross-layer optimization," *IEEE Trans. Veh. Technol.*, vol. 58, no. 4, pp. 1887–1903, May 2009.
- [9] Y. Zhang, F. Fu, and M. van der Schaar, "On-line learning and optimization for wireless video transmission," *IEEE Trans. Signal Process.*, vol. 58, no. 6, pp. 3108–3124, Jun. 2010.
- [10] F. Fu and M. van der Schaar, "A systematic framework for dynamically optimizing multi-user wireless video transmission," *IEEE J. Sel. Areas Commun.*, vol. 28, no. 3, pp. 308–320, Apr. 2010.
- [11] F. Fu and M. van der Schaar, "Structural solutions for dynamic scheduling in wireless multimedia transmission," *IEEE Trans. Circuits Syst. Video Technol.*, vol. 22, no. 5, pp. 727–739, May 2012.
- [12] C. Chen, R. W. Heath, A. C. Bovik, and G. de Veciana, "Adaptive policies for real-time video transmission: A Markov decision process framework," in *Proc. 18th IEEE Int. Conf. Image Process.*, Sep. 2011, pp. 2249–2252.
- [13] D. Love, R. W., Jr. Heath, W. Santipach, and M. Honig, "What is the value of limited feedback for MIMO channels?," *IEEE Commun. Mag.*, vol. 42, no. 10, pp. 54–59, Oct. 2004.
- [14] D. Love, R. Heath, V. Lau, D. Gesbert, B. Rao, and M. Andrews, "An overview of limited feedback in wireless communication systems," *IEEE J. Sel. Areas Commun.*, vol. 26, no. 8, pp. 1341–1365, Oct. 2008.
- [15] 3GPP, "Further advancements for E-UTRA physical layer aspects," 3rd Generation Partnership Project (3GPP), TR 36.814, 2010.
- [16] N. Changuel, B. Sayadi, and M. Kieffer, "Online learning for QoE-based video streaming to mobile receivers," in *Proc. Global Commun. Conf.*, Dec. 2012, pp. 1319–1324.
- [17] Q. Zhang and S. A. Kassam, "Finite-state Markov model for Rayleigh fading channels," *IEEE Trans. Commun.*, vol. 47, no. 11, pp. 1688–1692, Nov. 1999.
- [18] H. S. Wang and P.-C. Chang, "On verifying the first-order Markovian assumption for a Rayleigh fading channel model," *IEEE Trans. Veh. Technol.*, vol. 45, no. 2, pp. 353–357, May 1996.
- [19] H.-P. Lin and M.-J. Tseng, "Two-layer multistate Markov model for modeling a 1.8 GHz narrow-band wireless propagation channel in urban Taipei city," *IEEE Trans. Veh. Technol.*, vol. 54, no. 2, pp. 435–446, Mar. 2005.
- [20] T. Su, H. Ling, and W. J. Vogel, "Markov modeling of slow fading in wireless mobile channels at 1.9 GHz," *IEEE Trans. Antennas Propag.*, vol. 46, no. 6, pp. 947–948, Jun. 1998.
- [21] J. Sun, W. Gao, D. Zhao, and W. Li, "On rate-distortion modeling and extraction of H.264/SVC fine-granular scalable video," *IEEE Trans. Circuits Syst. Video Technol.*, vol. 19, no. 3, pp. 323–336, Mar. 2009.
- [22] C. Chen, R. W. Heath, Jr., A. C. Bovik, and G. de Veciana. (2011). "Markov decision model for perceptually optimized video scheduling." Tech. Rep. [Online]. Available: <https://webpace.utexas.edu/cc39488/pdf/report.pdf>
- [23] D. Bertsekas, *Dynamic Programming and Optimal Control*, vol. 2, 3rd ed. Belmont, MA: Athena Scientific, 2005.
- [24] Test sequences. (2012) [Online]. Available: <http://trace.eas.asu.edu/yuv/>
- [25] J. Reichel, S. Schwarz, and M. Wien, "Joint scalable video model 11 (JSVM 11)," Joint Video Team, Doc. JVT-X202, Jul. 2007.
- [26] K. Seshadrinathan, R. Soundararajan, A. C. Bovik, and L. K. Cormack, "Study of subjective and objective quality assessment of video," *IEEE Trans. Image Process.*, vol. 19, no. 6, pp. 1427–1441, Jun. 2010.
- [27] LIVE Image Quality Assessment Database. (2006) [Online]. Available: <http://live.ece.utexas.edu/research/quality/subjective.htm>
- [28] S. M. Pandit and S. M. Wu, *Time-Series and System Analysis With Application*. New York: Wiley, 1983.
- [29] M. Neuts, *Matrix-Geometric Solutions in Stochastic Models: An Algorithm Approach*. Baltimore, MD: The Johns Hopkins Univ. Press, 1981.



Chao Chen (S'11) received the B.E. and M.S. degrees in electrical engineering from Tsinghua University, Beijing, China, in 2006 and 2009, respectively. He is currently pursuing the Ph.D. degree in electrical and computer engineering at the University of Texas at Austin, Austin, TX, USA.

In 2009, he joined the Wireless Systems Innovation Laboratory and the Laboratory for Image & Video Engineering, The University of Texas at Austin, where he is currently involved in research on video quality assessment and wireless video communication. In 2012, he was an Intern at Qualcomm Inc., where he developed a nonreference video quality assessment method. His current research interests include stochastic control, system identification, and network resource allocation.



Robert W. Heath Jr. (S'96–M'01–SM'06–F'11) received the B.S. and M.S. degrees from the University of Virginia, Charlottesville, VA, USA, in 1996 and 1997, respectively, and the Ph.D. degree from Stanford University, Stanford, CA, USA, in 2002, all in electrical engineering.

From 1998 to 2001, he was a Senior Member of the Technical Staff and then a Senior Consultant at Iospan Wireless Inc., San Jose, CA, where he was involved in research on the design and implementation of the physical and link layers of the first commercial multiple-input and multiple-output (MIMO) orthogonal frequency-division multiplexing communication system. Since January 2002, he has been with the Department of Electrical and Computer Engineering, The University of Texas at Austin, Austin, where he is currently a Professor and the Director of the Wireless Networking and Communications Group. He is also the President and Chief Executive Officer at MIMO Wireless Inc., and the Chief Innovation Officer at Kuma Signals LLC. His research interests include several aspects of wireless communication and signal processing: limited feedback techniques, multiuser networking, multiuser and multicell MIMO, interference alignment, adaptive video transmission, manifold signal processing, and millimeter wave communication techniques.

Dr. Heath has been an Editor for the IEEE TRANSACTIONS ON COMMUNICATION, an Associate Editor for the IEEE TRANSACTIONS ON VEHICULAR TECHNOLOGY, a lead Guest Editor for the *IEEE Journal on Selected Areas in Communications* special issue on limited feedback communication, and a lead Guest Editor of the *IEEE Journal on Selected Topics in Signal Processing* special issue on Heterogenous Networks. He currently serves on the steering committee of the IEEE TRANSACTIONS ON WIRELESS COMMUNICATIONS. He was a member of the Signal Processing for Communications Technical Committee of the IEEE Signal Processing Society. He currently serves as the Chair of the Communications Technical Theory Committee of the IEEE Communications Society. He was the Technical Co-Chair for the 2007 Fall Vehicular Technology Conference (VTC), the General Chair of the 2008 Communication Theory Workshop, the General Co-Chair, Technical Co-Chair, and Co-Organizer of the 2009 IEEE Signal Processing for Wireless Communications Workshop, the local Co-Organizer for the 2009 IEEE International Workshop on Computational Advances in Multi-Sensor Adaptive Processing Conference, the Technical Co-Chair for the 2010 IEEE International Symposium on Information Theory, the Technical Chair for the 2011 Asilomar Conference on Signals, Systems, and Computers, the General Chair for the 2013 Asilomar Conference on Signals, Systems, and Computers, the General Co-Chair for the 2013 IEEE Global Conference on Signal and Information Processing, and the Technical Co-Chair for the 2014 IEEE Global Telecommunications (GLOBECOM) Conference. He was the co-author of publications that have won Best Student Paper Awards at the IEEE VTC 2006 Spring, the International Symposium on Wireless Personal Multimedia Communications 2006, the IEEE GLOBECOM 2006, the IEEE VTC 2007 Spring, and the IEEE Radio and Wireless Symposium 2009, as well as the corecipient of the Grand Prize in the 2008 WinTech WinCool Demo Contest. He was the corecipient of the 2010 *EURASIP Journal on Wireless Communications and Networking* Best Paper Award. He was a 2003 Frontiers in Education New Faculty Fellow. He is a recipient of the David and Doris Lybarger Endowed Faculty Fellowship in Engineering, a licensed Amateur Radio Operator, and a registered Professional Engineer in Texas.



Alan C. Bovik (F'96) received the B.S. degree in computer engineering in 1980, and the M.S. and Ph.D. degrees in electrical and computer engineering in 1982 and 1984, respectively, all from the University of Illinois at Urbana-Champaign, Urbana, IL, USA.

He is the Curry/Cullen Trust Endowed Chair Professor at The University of Texas at Austin, Austin, TX, USA, where he is the Director of the Laboratory for Image and Video Engineering. He is a faculty member in the Department of Electrical and

Computer Engineering and the Center for Perceptual Systems in the Institute for Neuroscience. His several books include the recent companion volumes *The Essential Guides to Image and Video Processing* (New York: Academic, 2009). His current research interests include image and video processing, computational vision, and visual perception. He has published more than 650 technical articles in these areas and holds two U.S. patents.

Dr. Bovik was named the Imaging Scientist 2011 by the Society of Photo-Optical and Instrumentation Engineers (SPIE)/Imaging Science and Technology. He has also received a number of major awards from the IEEE Signal Processing Society, including the Best Paper Award in 2009, the Education Award in 2007, the Technical Achievement Award in 2005, and the Meritorious Service Award in 1998. He received the Hocott Award for Distinguished Engineering Research at the University of Texas at Austin, the Distinguished Alumni Award from the University of Illinois at Urbana-Champaign in 2008, the IEEE Third Millennium Medal in 2000, and two journal paper awards from the international Pattern Recognition Society in 1988 and 1993. He is a Fellow of the Optical Society of America, a Fellow of the SPIE, and a Fellow of the American Institute of Medical and Biomedical Engineering. He has been involved in numerous professional society activities, including the Board of Governors, the IEEE Signal Processing Society from 1996 to 1998, the Co-Founder and Editor-in-Chief of the IEEE TRANSACTIONS ON IMAGE PROCESSING from 1996 to 2002, the Editorial Board of the PROCEEDINGS OF THE IEEE from 1998 to 2004, and the Founding General Chairman of the 1st IEEE International Conference on Image Processing, Austin, TX, November 1994. Since 2003, he has been the Series Editor for Image, Video, and Multimedia Processing of the Morgan and Claypool Publishing Company. He is a registered Professional Engineer in the State of Texas, USA, and is a frequent consultant to legal, industrial, and academic institutions.



Gustavo de Veciana (S'88–M'94–SM'01–F'09) received the B.S., M.S., and Ph.D. degrees in electrical engineering from the University of California at Berkeley, Berkeley, CA, USA, in 1987, 1990, and 1993, respectively.

He is currently the Joe. J. King Professor in the Department of Electrical and Computer Engineering, The University of Texas at Austin, Austin, TX, USA, where from 2003 to 2007, he was the Director and Associate Director of the Wireless Networking and Communications Group. His current research

interest is focused on the analysis and design of wireless and wireline telecommunication networks, architectures and protocols to support sensing and pervasive computing, applied probability, and queuing theory.

Dr. de Veciana was the Editor for the IEEE/ACM TRANSACTIONS ON NETWORKING. He was a recipient of the National Science Foundation CAREER Award in 1996, the corecipient of the IEEE William McCalla Best Paper Award at the International Conference on Computer-Aided Design in 2000, the corecipient of the Best Paper in ACM Transactions on Design Automation of Electronic Systems from January 2002 to 2004, the corecipient of the Best Paper in the 22nd International Teletraffic Congress in 2010, and the corecipient of the Best Paper at the ACM International Conference on Modeling, Analysis and Simulation of Wireless and Mobile Systems in 2010. He is on the Technical Advisory Board of the Institutos Madrilenes de Estudios Avanzados Networks.